Received: 24 June 2023 | Revised: 1 November 2023 | Accepted: 8 November 2023

DOI: 10.1111/cbdd.14400

RESEARCH ARTICLE

WILEY

Design and synthesis of imidazo[1,2-*a*]pyridine-chalcone conjugates as antikinetoplastid agents

Devesh S. Agarwal[1] | **Richard M. Beteck**[1] | **Kayhan Ilbeigi**[2] | **Guy Caljon**[2] | **Lesetja J. Legoabe**[1]

[1]Centre of Excellence for Pharmaceutical Sciences, North-West University, Potchefstroom, South Africa

[2]Laboratory of Microbiology, Parasitology and Hygiene, Infla-med Centre of Excellence, University of Antwerp, Antwerp, Belgium

Correspondence
Lesetja J. Legoabe, Centre of Excellence for Pharmaceutical Sciences, North-West University, Potchefstroom 2520, South Africa.
Email: lesetja.legoabe@nwu.ac.za

Guy Caljon, Laboratory of Microbiology, Parasitology and Hygiene, Infla-med Centre of Excellence, University of Antwerp, Antwerp 2610, Belgium.
Email: guy.caljon@uantwerpen.be

Abstract

A library of imidazo[1,2-a]pyridine-appended chalcones were synthesized and characterized using ^{1}H NMR, ^{13}C NMR and HRMS. The synthesized analogues were screened for their antikinetoplastid activity against *Trypanosoma cruzi*, *Trypanosoma brucei brucei*, *Trypanosoma brucei rhodesiense* and *Leishmania infantum*. The analogues were also tested for their cytotoxicity activity against human lung fibroblasts and primary mouse macrophages. Among all screened derivatives, **7f** was found to be the most active against *T. cruzi* and *T. b. brucei* exhibiting IC_{50} values of 8.5 and 1.35 μM, respectively. Against *T. b. rhodesiense*, **7e** was found to be the most active with an IC_{50} value of 1.13 μM. All synthesized active analogues were found to be non-cytotoxic against MRC-5 and PMM with selectivity indices of up to more than 50.

KEYWORDS

antikinetoplastid, chalcone, drug likeliness properties, imidazo[1,2-*a*]pyridine, neglected tropical diseases (NTDs), *Trypanosoma brucei brucei*, *Trypanosoma brucei rhodesiense*

1 | INTRODUCTION

Kinetoplastids represent a class of flagellated eukaryotic parasites and the uniflagellate trypanosomatids including the *Leishmania* and *Trypanosoma* species (Deschamps et al., 2011; Molyneux et al., 2017; Povelones, 2014; Stuart et al., 2008). The distinguished feature associated with this group is the presence of a kinetoplast (mitochondrial structure containing circular DNA) (Davis et al., 2003). Members of this group are responsible for neglected tropical diseases (NTDs), including human African trypanosomiasis (HAT; caused by *Trypanosoma brucei*), Chagas disease (caused by *Trypanosoma cruzi*) and leishmaniasis (caused by several *Leishmania* species; Deschamps et al., 2011; Molyneux et al., 2017; Stuart et al., 2008). According to the World Health Organization (WHO), NTDs are associated with poverty, weak immune systems, poor housing conditions, malnutrition, lack of resources and population displacement (Pillay-van Wyk & Bradshaw, 2017). Drugs for the treatment of the aforementioned NTDs include Amphotericin B (AmB) and its liposomal form (AmBisome), paromomycin, benznidazole, nifurtimox, antimony compounds (sodium stibogluconate and meglumine antimoniate) and miltefosine (Zulfiqar et al., 2017), nifurtimox–eflornithine combination and fexinidazole, an oral drug for advanced-stage HAT (Patterson & Wyllie, 2014; Wyllie et al., 2012; Zulfiqar et al., 2017). Nifurtimox and fexinidazole share a common

bioactivation mechanism, with the possible drawback of the risk of cross-resistance. General shortcomings associated with the listed drugs include toxic side effects, appearance of resistant strains and low efficacy (Croft & Olliaro, 2011; De Rycker et al., 2018; Field et al., 2017; Lidani et al., 2019).

Imidazo[1,2-*a*]pyridine is a diversified scaffold present in various marketed drugs such as alpidem, zolpidem (Harrison & Keating, 2005), optically active GSK812397, necopidem and zolimidine. In addition, its derivatives have exhibited various biological activities such as anticancer, analgesic, antipyretic, antiviral including anti-HIV activities, liver X receptor (LXR) agonists (Singhaus et al., 2010), γ-secretase modulators (GSMs) (Bischoff et al., 2012), positive allosteric modulators (PAMs) of metabotropic glutamate 2 receptor (Tresadern et al., 2010) and GABAA$\alpha 2$/$\alpha 3$ agonists (Almirante et al., 1965; Coulibaly et al., 2023; Deep et al., 2017; Devi et al., 2016; Goodacre et al., 2006).

Additionally, chalcones are naturally occurring and synthetic compounds. They possess a broad range of pharmacological properties such as anticancer, amoebicidal, antiviral, antibacterial, anthelmintic, antiulcer, insecticidal, antiprotozoal, cytotoxic and immunosuppressive activities (Elkanzi et al., 2022; Rammohan et al., 2020; Salehi et al., 2021).

With respect to the kinetoplastid agents, extensive research has been fuelled towards the development of novel and more efficient agents. For instance, in 2014, Nava-Zuazo et al. reported synthesis of 2-acylamino-5-nitro-1,3-thiazoles (**I**, Figure 1) and their antiprotozoal activity against *Giardia intestinalis*, *Trichomonas vaginalis*, *Leishmania amazonensis* and *T. cruzi*. Among all the synthesized derivatives, the most potent derivatives showed an IC_{50} value of 0.010 ± 0.001 and 0.010 ± 0.003 μM against *G. intestinalis* and *T. vaginalis*, respectively (**I**, Figure 1; Nava-Zuazo et al., 2014). Bhambra et al. reported synthesis of pyridylchalcones as antitrypanosomal agents against *T. b. rhodesiense*. The most active analogue **II** (Figure 1) was found to possess an IC_{50} value of 0.29 μM against *T. b. rhodesiense* (Bhambra et al., 2017). Vanelle et al. have extensively worked on nitroimidazopyridine analogues as antikinetoplastid agents. For instance, in 2013, the authors reported the synthesis of a series of 3-nitroimidazo[1,2-*a*]pyridine and tested their activity against *L. donovani*. The most active compound (**III**, Figure 1) was found to possess an IC_{50} value of 1.8 ± 0.8 μM (Castera-Ducros et al., 2013). Continuing their efforts, in 2018 the authors reported synthesis of 8-Aryl-6-chloro-3-nitro-2-(phenylsulfonylmethyl)imidazo[1,2-*a*]pyridines (**IV**, Figure 1) and studied their antitrypanosomal activity.

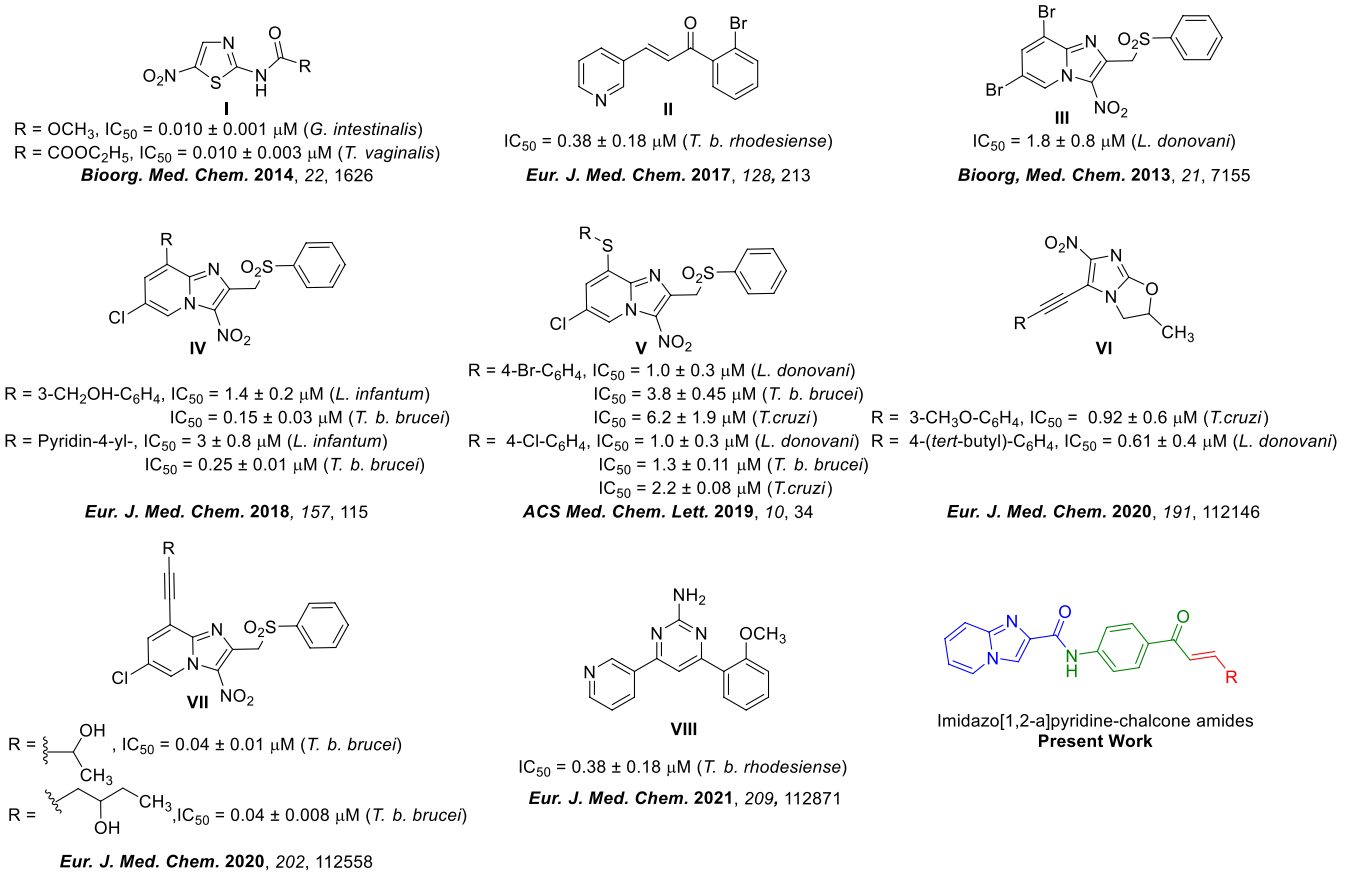

FIGURE 1 Selected literature reports of antikinetoplastid agents.

Two hit compounds were obtained from the series with an IC_{50} value in the range of 1.4–3 μM and 0.15–0.25 μM against *L. infantum* and *T. b. brucei*, respectively Figure 1 (Fersing, Boudot, et al., 2018). In the same year, they also synthesized 3-nitroimidazo[1,2-*a*]-pyridine derivatives, bearing a phenylthio (or benzylthio) moiety (**V**, Figure 1), and studied their activity against *T. cruzi* and *L. donovani* (Fersing, Basmaciyan, et al., 2018). In 2020, the same group reported synthesis of 5-substituted 6-nitroimidazo-oxazoles (**VI**, Figure 1) as antikinetoplastid agents against *L. donovani* and *T. cruzi*. Among all the analogues, one was found to be active against *T.cruzi* with an IC_{50} value of 0.92 ± 0.6 μM and another one was found active against *L. donovani* with an IC_{50} value of 0.61 ± 0.4 μM (**VI**, Figure 1; Mathias et al., 2020). Subsequently, the same group reported the synthesis of 8-alkynyl-3-nitroimidazopyridines (**VII**, Figure 1) and studied their activity against *T. b. brucei* and *T. cruzi*. The best compounds were found to possess an IC_{50} value of 0.04 ± 0.01 and 0.04 ± 0.008 μM against *T. b. brucei* (**VII**, Figure 1; Fersing et al., 2020). In 2021, Robinson et al. reported the synthesis of 4-phenyl-6-(pyridin-3-yl) pyrimidines analogues as antitrypanosomal against *T. b. rhodesiense*. Among all the analogues synthesized, the best compound (**VIII**, Figure 1) was found to possess an IC_{50} value of 0.38 ± 0.18 μM against *T. b. rhodesiense* (Figure 1; Robinson et al., 2021). However, in this battle, imidazo[1,2-a]pyridine-appended chalcones are not yet explored.

In context of the above discussion and in our effort to develop novel antikinetoplastid agents, we herein report the synthesis of imidazo[1,2-a]pyridine-chalcone amides (**7a–l**, Scheme 1). The synthesized analogues (**5**, **7a–l**) were examined for their antikinetoplastid activity against *T. cruzi*, *T. b. brucei*, *T. b. rhodesiense* and *Leishmania infantum*. In addition, the synthesized analogues were also tested for their cytotoxicity against human lung fibroblasts (MRC-5) and primary mouse macrophages (PMMs).

2 | RESULT AND DISCUSSION

2.1 | Chemistry

In the present study, we synthesized imidazo[1,2-a] pyridine-appended chalcones via amidic bond (**7a–l**, Scheme 1). The synthesis commences with the reaction of 2-amino pyridine (**1**) with bromo pyruvic acid (**2**) in ethanol at 80°C to give imidazo[1,2-*a*]pyridine-2-carboxylic acid (**3**) in 72% yield (Reddyrajula & Dalimba, 2019). Followed by the coupling of 1-(4-aminophenyl)ethan-1-one (**4**) with imidazo[1,2-*a*]pyridine-2-carboxylic acid (**3**) using EDC.HCl/HOBt in DMF at rt to give *N*-(4-acetylphenyl)imidazo[1,2-*a*]pyridine-2-carboxamide (**5**) in 72% yield (Agarwal et al., 2016).

Appearance of the amide NH proton at δ 10.62 and methyl group (-$COCH_3$) proton at δ 2.55 in ^{1}H NMR and the corresponding carbonyl group (C=O) of amide and ketone at δ 161.2 and 196.7, respectively on the ^{13}C NMR confirmed the formation of **5**.

Finally, *N*-(4-acetylphenyl)imidazo[1,2-*a*]pyridine-2-carboxamide (**5**) was reacted with different aldehydes (**6**) in EtOH using 2 N NaOH to give corresponding (*E*)-*N*-(4-(3-(aryl)acryloyl)phenyl)imidazo[1,2-*a*]pyridine-2-carboxamides (**7a–l**) in excellent yield. The structure of all new molecules was characterized using ^{1}H NMR, ^{13}C NMR and HRMS (Data S1).

2.2 | Pharmacology

The antikinetoplastid activity of all the synthesized derivatives **5**, **7a–l** was investigated against *T. cruzi*, *T. b. brucei*, *T. b. rhodesiense* and *L. infantum*. In addition, the synthesized derivatives **5** and **7a–l** were also tested for their cytotoxicity against MRC-5 and PMM. Among all the derivatives, **7f** was found to be most active against *T. cruzi* with an IC_{50} value of 0.68 μM. Analogue **7f** shows a

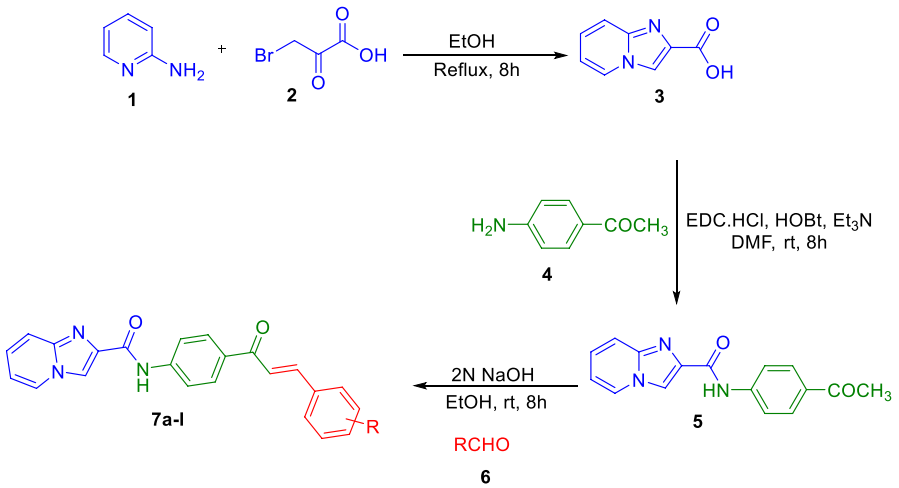

SCHEME 1 Synthesis of (*E*)-*N*-(4-(3-(aryl)acryloyl)phenyl)imidazo[1,2-*a*] pyridine-2-carboxamides (**7a–l**).

twofold increase in activity with respect to the reference drug benznidazole with an IC_{50} value of 1.35 μM. With respect to the activity against *T. b. brucei*, *mono* electron-donating group substituted product, for example, **7a** and **7b**, were found to be active with an IC_{50} values of 6.40 and 5.35 μM, respectively. Halogen-substituted derivatives **7e–k** were found to exhibit IC_{50} values ranging from 1.28 to 57.97 μM. The mono-halogenated derivatives **7e–j** and 2- and 3-substituted derivatives **7f**, **7g** and **7i** were found to be more active than their 4-substituted analogues **7e**, **7h** and **7j**. For instance, **7f** and **7g** were found to be the most active with an IC_{50} values of 1.28 and 1.35 μM, respectively as compared to their 4-substituted counterpart **7h** with an IC_{50} value of 57.97 μM. Compound **7i** was also found to be active with an IC_{50} value of 2.20 μM as compared to compound **7j** with an IC_{50} value of 28.04 μM. Compound **7k** also demonstrated low micromolar activity with an IC_{50} value of 2.52 μM. Suramine was used as reference drug against *T. b. brucei* with an IC_{50} value of 0.04 μM.

All synthesized derivatives were also tested against *T. b. rhodesiense*, revealing that among all methyl- and methoxy-substituted derivatives **7a–d**, we found **7a** to be most active with an IC_{50} value of 2.31 μM. Among the mono-halogen-substituted derivatives, **7e–j** were found to be active with IC_{50} values in the range of 1–12 μM.

Against *L. infantum*, all derivatives **5**, **7a–l** were found to be inactive with IC_{50} values of >64.00 μM as compared to miltefosine (IC_{50} = 7.13 μM) which was included as reference.

With respect to the cytotoxicity against MRC-5, all derivatives **5**, **7a–l** were found to be non-cytotoxic with an IC_{50} value of >64.00 μM as compared to tamoxifen (IC_{50} = 10.79 μM) except for **7c** and **7j** which possess IC_{50} values of 45.25 and 32.00 μM, respectively. Concerning cytotoxicity against PMM, all the derivatives **5**, **7a-l** were found to be non-cytotoxic with IC_{50} values of >64.00 μM (Table 1).

2.3 | Drug likeliness properties and drug score predictions

Computational studies of compounds **5** and **7a–l** were carried out for predicting the absorption, distribution, metabolism and excretion (ADME) properties (Table 2). Physiochemical properties of the molecules were also predicted using Lipinski's rule of five, drug likeness score and percentage absorption (Table 2). ADME properties were calculated online using Molinspiration cheminformatics software (Agarwal

TABLE 1 Antikinetoplastid and cytotoxic activities (IC_{50}, μM) of synthesized compounds (**5**, **7a–l**).

		IC_{50} (μM)					
Compd	**R**	***T. cruz.***	***T. b. bruc.***	***T. b. rhod.***	***L. inf.***	**MRC-5**[a]	**PMM**
5	–	>64.00	>64.00	40.32	>64.00	>64.00	>64.00
7a	2-CH_3	>64.00	**6.40**	**2.31**	>64.00	>64.00	>64.00
7b	3-OCH_3	>64.00	**5.35**	**9.19**	>64.00	>64.00	>64.00
7c	2,4-di-OCH_3	>64.00	>64.00	38.40	>64.00	**45.25**	>64.00
7d	2,5-di-OCH_3	>64.00	12.93	**6.35**	>64.00	>64.00	>64.00
7e	4-Br	>64.00	22.63	**1.13**	>64.00	>64.00	>64.00
7f	2-Cl	**8.5 ± 12**	**1.57 ± 0.03**	**1.35 ± 0.03**	>64.00	>64.00	>64.00
7g	3-Cl	**32.34**	**1.35**	**1.41**	>64.00	>64.00	>64.00
7h	4-Cl	>64.00	57.97	**1.79**	>64.00	>64.00	>64.00
7i	3-F	>64.00	**2.20**	**1.66**	>64.00	>64.00	>64.00
7j	4-F	>64.00	28.04	12.82	>64.00	**32.00**	>64.00
7k	3,4-di-Cl	>64.00	**2.52**	20.25	>64.00	>64.00	>64.00
7l	4-NO_2	>64.00	–[b]	38.34	>64.00	>64.00	>64.00
	Benznidazole	**1.35**	–	–	–	–	–
	Suramine	–	**0.04**	**0.05**	–	–	–
	Miltefosine	–	–	–	**7.13**	–	–
	Tamoxifen	–	–	–	–	**10.79**	–

Abbreviations: PMM, primary mouse microphages; *T. b. bruc.*, *Trypanosoma brucei brucei*; *T. b. rhod.*, *Trypanosoma brucei rhodesiense*; *T. cruz.*, *Trypanosoma cruzi*; *L. inf.*, *Leishmania infantum*.

[a]Lung fibroblast.

[b]No activity.

et al., 2016; Reddy et al., 2018), while the drug likeness scores were calculated online using MolSoft software (Agarwal, Krishna, et al., 2018; Agarwal, Singh, et al., 2018; Reddy et al., 2018). In addition, all the derivatives were also evaluated for percentage absorption (% ABS) using the formula $\%ABS = 109 - (0.345 \times TPSA)$ (Zhao et al., 2002). It was observed that all synthesized derivatives **5** and **7a–l** were found to have TPSA less than 160 $Å^2$ but >40 $Å^2$ indicating that molecules to have a potential for good intestinal absorption property as compared to their blood–brain barrier (BBB) penetration ability (Table 2). Compound **7e**, the most active compound against *T. b. rhodesiense*, was found to possess TPSA of **63.48** $Å^2$ and **7f** most active against *T. cruzi* and *T. b. brucei* was found to possess TPSA of **63.48** $Å^2$ (Table 2). Compounds **7e** and **7f** also possessed a positive drug likeliness score of 0.73 and 0.58, respectively, which predicts them as good drug candidates (Table 2).

3 | CONCLUSION

In summary, we have designed and synthesised a series of imidazo[1,2-a]pyridine-chalcones in satisfactory yield. All synthesized derivatives were characterized using different analytical techniques such as ^{1}H NMR, ^{13}C NMR and HRMS. The synthesized analogues were evaluated for their antikinetoplastid activity against *T. cruzi*, *T. b. brucei*, *T. b. rhodesiense* and *L. infantum*. The compounds were also tested for cytotoxicity against MRC-5 and PMM. Among all analogues tested, **7f** was found to be the most active against *T. cruzi* and *T. b. brucei* with IC_{50} values of 8.5 and 1.35 μM, respectively. With respect to cytotoxicity against the human lung fibroblast cell line (MRC-5) and PMM, all active analogues were found to be non-cytotoxic. These results identify the synthesized analogues as hits against *T. cruzi*, *T. b. brucei* and *T. b. rhodesiense*. Additional follow-up studies are warranted to further explore the imidazo[1,2-*a*]pyridine-chalcone hit series and identify the most promising candidates for progression to in vivo models.

4 | MATERIALS AND METHODS

4.1 | General

All the chemicals were purchased from various chemical suppliers including Sigma-Aldrich, Ace, Rochelle and Ambeed and used without further purification. The progress of the reactions was monitored using thin layer chromatography (TLC) on Merck $60F_{254}$ silica gel plates supported on 0.20-mm-thick aluminium sheets. Nuclear magnetic resonance (NMR) spectra were recorded on a Bruker Avance III 600 spectrophotometer at 600 MHz (for ^{1}H) and 150 MHz (for ^{13}C). The ^{1} H NMR chemical shifts (δ) were reported in parts per million (ppm), and were measured relative to residual deuterochloroform ($CDCl_3$) (7.26 ppm) or DMSO-d_6 (2.5 ppm). The ^{13}C NMR spectra were reported in ppm relative to deuterochloroform ($CDCl_3$) (77.0 ppm) or DMSO-d_6 (39.5 ppm). All coupling constants J were reported in Hz. The following abbreviations were used to describe peak splitting patterns: s = singlet, d = doublet, t = triplet, dd = doublet of doublet, m = multiplet and brs = broad singlet. High-resolution mass spectra were recorded on an Agilent Technologies micrOTOF-Q II 2010390 by using atmospheric pressure chemical ionization (APCI) in positive ion mode. Melting points were obtained using Buchi B-545 melting point apparatus and are uncorrected. imidazo[1,2-*a*]pyridine-2-carboxylic acid was synthesized according to the reported literature (Reddyrajula & Dalimba, 2019).

4.2 | Chemistry

4.2.1 | General procedure for the synthesis of N-(4-acetylphenyl)imidazo[1,2-a]pyridine-2-carboxamide (5)

To a stirred solution of imidazo[1,2-*a*]pyridine-2-carboxylic acid (**3**, 3 g, 1 mmol) in DMF (5 mL), triethylamine (6.48 mL, 2.5 mmol) was added at rt and subsequently, EDC.HCl (5.16 g, 1.5 mmol) and HOBt (2.75 g, 1 mmol) were added. The reaction was stirred at rt for 0.5 h. Thereafter, 1-(4-aminophenyl)ethan-1-one (**4**, 3.0 g, 1.2 mmol) was added and the reaction was stirred at rt for 8 h. The progress of the reaction was monitored by TLC. After the completion of the reaction, it was quenched by adding water and the mixture extracted using ethyl acetate (100 mL × 2) twice. The combined organic layer was dried over anhydrous Na_2SO_4 and concentrated under reduced pressure to give crude product. The crude product was purified using silica column chromatography with EA/Hexane (2:5) to obtain pure product (**5**) as off-white solid.

White solid, 3 g (72% yield), mp: 220–221°C, ^{1}H NMR (600 MHz, DMSO-d_6) δ 10.62 (s, 1H), 8.63 (d, J = 6.8 Hz, 1H), 8.57 (s, 1H), 8.07 (d, J = 8.7 Hz, 2H), 7.96 (d, J = 8.7 Hz, 2H), 7.67 (d, J = 9.2 Hz, 1H), 7.40 (dd, J = 8.4, 7.4 Hz, 1H), 7.03 (t, J = 6.8 Hz, 1H), 2.55 (s, 3H). ^{13}C NMR (150 MHz, DMSO-d_6) δ 196.7, 161.3, 144.0, 143.2, 139.1, 132.0, 129.3, 127.8, 126.9, 119.4, 117.4, 116.0, 113.6, 26.5. HRMS (APCI): m/z calcd for $C_{16}H_{14}N_3O_2$ $[M + H]^+$ 280.1081, found 280.1078.

TABLE 2 Drug likeliness properties, % ABS and drug score predictions of synthesized compounds (**5**, **7a–l**).

Compd	miLogP	TPSA	natoms	MW	nHBA (O & N)	nHBD (OH & NH)	nviolations	nrotb	Volume	% ABS[a]	Drug likeness score[b]
5	2.33	63.48	21	279.30	5	1	0	3	247.59	87.09	0.51
7a	4.53	63.48	29	381.44	5	1	0	5	346.41	87.09	0.46
7b	4.34	72.71	30	397.43	6	1	0	6	355.39	83.91	0.94
7c	4.17	81.94	32	427.46	7	1	0	7	380.94	80.73	0.43
7d	4.17	81.94	32	427.46	7	1	0	7	380.94	80.73	0.40
7e	**5.11**	**63.48**	**29**	**446.30**	**5**	**1**	**1**	**5**	**347.74**	**87.09**	**0.73**
7f	**4.75**	**63.48**	**29**	**401.85**	**5**	**1**	**0**	**5**	**343.38**	**87.09**	**0.58**
7 g	4.96	63.48	29	401.85	5	1	0	5	343.38	87.09	0.89
7 h	4.98	63.48	29	401.85	5	1	0	5	343.38	87.09	1.03
7i	4.44	63.48	29	385.40	5	1	0	5	334.78	87.09	0.82
7j	4.47	63.48	29	385.40	5	1	0	5	334.78	87.09	0.89
7 k	5.41	63.48	30	436.30	5	1	1	5	356.92	87.09	0.79
7 L	4.26	109.30	31	412.40	8	1	0	6	353.18	71.29	0.38

Abbreviations: miLogP, logarithm of compound partition coefficient between *n*-octanol and water; MW, molecular weight of the molecules; natoms, number of atoms in the molecule; nHBA, number of hydrogen bond acceptors; nHBD, number of hydrogen bond donors; nviolations, nrotb, number of rotatable bonds; TPSA, topological polar surface area; volume, volume of the molecule.

[a]Percentage absorption calculated using the formula $\%ABS = 109 - (0.345 \times TPSA)$.

[b]Drug-likeness score calculated using molsoft.

4.2.2 | General procedure for the synthesis of (E)-N-(4-(3-(aryl/hetroaryl)acryloyl)phenyl) imidazo[1,2-a]pyridine-2-carboxamide (**7a–l**)

To a stirred solution of *N*-(4-acetylphenyl)imidazo[1,2-*a*] pyridine-2-carboxamide (**5**, 150 mg, 1 mmol) in ethanol (10 mL), 2 N NaOH (2 mL) was added at rt and the reaction was stirred for 10 min. Subsequently, different aldehydes (**6**, 1.2 mmol) were added, and the reaction was stirred at rt for 8 h. The progress of the reaction was monitored by TLC. After completion of the reaction, the reaction mixture was quenched by adding water (20 mL) and the resulted precipitate was filtered under suction. The resulted precipitate was consequently washed with water (10 mL) and finally recrystallized with ethanol (3 mL) to obtain pure products **7a-l** in excellent yield.

4.2.2.1 | *(E)-N-(4-(3-(o-Tolyl)acryloyl)phenyl) imidazo[1,2-a]pyridine-2-carboxamide (**7a**)*

Off-white solid, 149 mg (73% yield), mp: 202–203°C, ^{1}H NMR (600 MHz, DMSO-d_6) δ 10.68 (s, 1H), 8.64 (d, J = 6.5 Hz, 1H), 8.59 (s, 1H), 8.19 (d, J = 8.4 Hz, 2H), 8.14 (d, J = 8.3 Hz, 2H), 8.05–7.95 (m, 2H), 7.86 (d, J = 15.4 Hz, 1H), 7.68 (d, J = 9.0 Hz, 1H), 7.44–7.39 (m, 1H), 7.38–7.24 (dd, J = 30.0, 6.9 Hz, 3H), 7.04 (t, J = 6.4 Hz, 1H), 2.45 (s, 3H). ^{13}C NMR (150 MHz, DMSO-d_6) δ 187.6, 161.3, 143.9, 143.3, 140.4, 139.1, 137.9, 133.4, 132.5, 130.8, 130.2, 129.7, 127.8, 126.9, 126.8, 126.4, 122.9, 119.5, 117.4, 116.0, 113.5, 19.4. HRMS (APCI): *m/z* calcd for $C_{24}H_{20}N_3O_2^+$ $[M + H]^+$ 382.1550, found 382.1541.

4.2.2.2 | *(E)-N-(4-(3-(3-Methoxyphenyl)acryloyl) phenyl)imidazo[1,2-a]pyridine-2-carboxamide (**7b**)*

Off-white solid, 151 mg (71% yield), mp: 209–210°C, ^{1}H NMR (600 MHz, DMSO-d_6) δ 10.68 (s, 1H), 8.64 (d, J = 6.8 Hz, 1H), 8.59 (s, 1H), 8.21 (d, J = 8.8 Hz, 2H), 8.15 (d, J = 8.7 Hz, 2H), 7.99 (d, J = 15.6 Hz, 1H), 7.74–7.64 (dd, J = 15.7, 12.4 Hz, 2H), 7.50 (s, 1H), 7.45–7.36 (m, 3H), 7.06–7.02 (m, 2H), 3.84 (s, 3H).^{13}C NMR (150 MHz, DMSO-d_6) δ 187.6, 161.3, 159.7, 143.9, 143.3, 139.1, 136.2, 132.5, 129.9, 129.7, 127.8, 126.8, 122.3, 121.7, 119.5, 117.4, 116.6, 116.0, 113.5, 113.2, 55.3. HRMS (APCI): *m/z* calcd for $C_{24}H_{20}N_3O_3^+$ $[M + H]^+$ 398.1499, found 398.1489.

4.2.2.3 | *(E)-N-(4-(3-(2,4-Dimethoxyphenyl)acryloyl) phenyl)imidazo[1,2-a]pyridine-2-carboxamide (**7c**)*

Off-white solid, 165 mg (72% yield), mp: 301–302°C, ^{1}H NMR (600 MHz, DMSO-d_6) δ 10.64 (s, 1H), 8.64 (d, J = 5.9 Hz, 1H), 8.59 (s, 1H), 8.12 (s, 3H), 7.99 (d, J = 15.5 Hz, 1H), 7.93 (d, J = 8.2 Hz, 1H), 7.79 (d, J = 15.7 Hz, 1H), 7.68 (d, J = 9.2 Hz, 1H), 7.43–7.38 (m, 1H), 7.05 (d, J = 5.7 Hz, 1H), 6.64 (d, J = 13.4 Hz, 3H), 3.91 (s, 3H), 3.85 (s, 3H). ^{13}C NMR (150 MHz, DMSO-d_6) δ 187.6, 163.0, 161.2, 159.9, 143.9, 143.0, 139.2, 138.1, 133.0, 130.0, 129.4, 127.8, 126.8, 119.5, 119.0, 117.4, 116.0, 115.9, 113.5, 112.7, 106.3, 98.3, 55.8, 55.5. HRMS (APCI): m/z calcd for $C_{25}H_{22}N_3O_3^+$ $[M + H]^+$ 428.1605, found 428.1615.

4.2.2.4 | *(E)-N-(4-(3-(2,5-Dimethoxyphenyl)acryloyl) phenyl)imidazo[1,2-a]pyridine-2-carboxamide (**7d**)*

Off-white solid, 165 mg (72% yield), mp: 167–168°C, ^{1}H NMR (600 MHz, DMSO-d_6) δ 10.68 (s, 1H), 8.64 (d, J = 6.5 Hz, 1H), 8.59 (s, 1H), 8.19 (d, J = 8.5 Hz, 2H), 8.15 (d, J = 8.4 Hz, 2H), 8.03 (d, J = 15.7 Hz, 1H), 7.94 (d, J = 15.7 Hz, 1H), 7.68 (d, J = 9.0 Hz, 1H), 7.57 (s, 1H), 7.45–7.36 (m, 1H), 7.04 (s, 3H), 3.85 (s, 3H), 3.81 (s, 3H). ^{13}C NMR (150 MHz, DMSO-d_6) 187.7, 161.2, 153.3, 152.7, 143.9, 143.2, 139.1, 137.6, 132.6, 129.6, 127.8, 126.7, 123.6, 122.0, 119.5, 118.0, 117.3, 115.9, 113.5, 113.0, 112.5, 56.2, 55.7. HRMS (APCI): m/z calcd for $C_{25}H_{22}N_3O_4^+$ $[M + H]^+$ 428.1605, found 428.1615.

4.2.2.5 | *(E)-N-(4-(3-(4-Bromophenyl)acryloyl) phenyl)imidazo[1,2-a]pyridine-2-carboxamide (**7e**)*

Off-white solid, 184 mg (77% yield), mp: 204–205°C, ^{1}H NMR (600 MHz, DMSO-d_6) δ 10.68 (s, 1H), 8.64 (d, J = 6.6 Hz, 1H), 8.58 (d, J = 7.5 Hz, 1H), 8.20 (d, J = 8.8 Hz, 2H), 8.15 (d, J = 8.7 Hz, 2H), 8.02 (d, J = 15.6 Hz, 1H), 7.87 (d, J = 8.4 Hz, 2H), 7.73–7.64 (m, 4H), 7.43–7.38 (m, 1H), 7.04 (dd, J = 8.3, 4.8 Hz, 1H). ^{13}C NMR (150 MHz, DMSO-d_6) δ 187.5, 161.2, 143.9, 143.3, 141.9, 139.1, 134.1, 132.4, 131.8, 130.7, 129.7, 129.2, 127.8, 126.7, 123.7, 122.9, 119.5, 117.3, 115.9, 113.5. HRMS (APCI): m/z calcd for $C_{23}H_{17}BrN_3O_2^+$ $[M + H]^+$ 446.0499, found 446.0506.

4.2.2.6 | *(E)-N-(4-(3-(2-Chlorophenyl)acryloyl) phenyl)imidazo[1,2-a]pyridine-2-carboxamide (**7f**)*

Off-white solid, 170 mg (79% yield), mp: 210–211°C, ^{1}H NMR (600 MHz, DMSO-d_6) δ 10.70 (s, 1H), 8.64 (d, J = 6.8 Hz, 1H), 8.59 (s, 1H), 8.24 (dd, J = 7.4, 1.9 Hz, 1H), 8.21 (d, J = 8.8 Hz, 2H), 8.16 (d, J = 8.8 Hz, 2H), 8.04 (s, 2H), 7.68 (d, J = 9.1 Hz, 1H), 7.58 (dd, J = 7.6, 1.5 Hz, 1H), 7.50–7.45 (m, 2H), 7.41 (dd, J = 8.5, 7.4 Hz, 1H), 7.04 (t, J = 6.7 Hz, 1H). ^{13}C NMR (150 MHz, DMSO-d_6) δ 187.4, 161.3, 143.9, 143.5, 139.1, 137.9, 134.3, 132.4, 132.2, 131.9, 130.0, 129.8, 128.6, 127.8, 127.7, 126.8, 124.8, 119.5, 117.4, 116.0, 113.5. HRMS (APCI): m/z calcd for $C_{23}H_{17}ClN_3O_2^+$ $[M + H]^+$ 402.1004, found 402.1004.

4.2.2.7 | *(E)-N-(4-(3-(3-Chlorophenyl)acryloyl) phenyl)imidazo[1,2-a]pyridine-2-carboxamide (**7 g**)*

Off-white solid, 164 mg (76% yield), mp: 208–209°C, ^{1}H NMR (600 MHz, DMSO-d_6) δ 10.68 (s, 1H), 8.64 (d, J = 6.8 Hz, 1H), 8.59 (s, 1H), 8.22 (d, J = 8.7 Hz, 2H), 8.15 (d, J = 8.8 Hz, 2H), 8.12–8.04 (m, 2H), 7.83 (d, J = 6.7 Hz, 1H), 7.74–7.65 (m, 2H), 7.52–7.46 (m, 2H), 7.43–7.37 (m, 1H),

7.04 (t, J = 6.6 Hz, 1H). ^{13}C NMR (150 MHz, DMSO-d_6) δ 187.4, 161.3, 143.9, 143.4, 141.6, 139.1, 137.1, 133.8, 132.3, 130.7, 130.0, 129.8, 127.9, 127.8, 126.8, 123.6, 119.5, 117.4, 116.0, 113.5. HRMS (APCI): m/z calcd for $C_{23}H_{17}ClN_3O_2^+$ $[M + H]^+$ 402.1004, found 402.0999.

4.2.2.8 | *(E)-N-(4-(3-(4-Chlorophenyl)acryloyl) phenyl)imidazo[1,2-a]pyridine-2-carboxamide (**7 h**)*

Off-white solid, 168 mg (78% yield), mp: 280–281°C, ^{1}H NMR (600 MHz, DMSO-d_6) δ 10.68 (s, 1H), 8.64 (d, J = 6.5 Hz, 1H), 8.59 (s, 1H), 8.20 (d, J = 8.6 Hz, 2H), 8.14 (d, J = 8.5 Hz, 2H), 8.01 (d, J = 15.6 Hz, 1H), 7.95 (d, J = 8.1 Hz, 2H), 7.75–7.65 (m, 2H), 7.53 (d, J = 8.2 Hz, 2H), 7.43–7.39 (m, 1H), 7.04 (t, J = 6.5 Hz, 1H).^{13}C NMR (150 MHz, DMSO-d_6) δ 187.5, 161.3, 143.4, 141.9, 139.1, 134.9, 132.4, 130.5, 129.7, 128.9, 127.8, 126.8, 122.8, 119.5, 117.4, 116.0, 113.6. HRMS (APCI): m/z calcd for $C_{23}H_{17}ClN_3O_2^+$ $[M + H]^+$ 402.1004, found 402.1007.

4.2.2.9 | *(E)-N-(4-(3-(3-Fluorophenyl)acryloyl) phenyl)imidazo[1,2-a]pyridine-2-carboxamide (**7i**)*

Off-white solid, 159 mg (77% yield), mp: 236–237°C, ^{1}H NMR (600 MHz, DMSO-d_6) δ 10.68 (s, 1H), 8.64 (d, J = 6.5 Hz, 1H), 8.59 (s, 1H), 8.21 (d, J = 8.4 Hz, 2H), 8.15 (d, J = 8.4 Hz, 2H), 8.05 (d, J = 15.6 Hz, 1H), 7.86 (d, J = 10.0 Hz, 1H), 7.75–7.65 (m, 3H), 7.50 (dd, J = 14.0, 7.4 Hz, 1H), 7.43–7.38 (m, 1H), 7.28 (t, J = 7.5 Hz, 1H), 7.04 (t, J = 6.4 Hz, 1H). ^{13}C NMR (150 MHz, DMSO-d_6) δ 187.5, 163.3, 161.7, 161.3, 143.9, 143.4, 141.8, 139.1, 137.40 (d, J = 8.0 Hz), 132.3, 130.8 (d, J = 8.5 Hz), 129.8, 127.8, 126.8, 125.5, 123.5, 119.5, 117.4, 116.0, 113.5. HRMS (APCI): m/z calcd for $C_{23}H_{17}FN_3O_2^+$ $[M + H]^+$ 386.1299, found 386.1313.

4.2.2.10 | *(E)-N-(4-(3-(4-Fluorophenyl)acryloyl) phenyl)imidazo[1,2-a]pyridine-2-carboxamide (**7j**)*

Off-white solid, 165 mg (80% yield), mp: 372–373°C, ^{1}H NMR (600 MHz, DMSO-d_6) δ 10.67 (s, 1H), 8.64 (d, J = 6.7 Hz, 1H), 8.59 (s, 1H), 8.19 (d, J = 8.6 Hz, 2H), 8.14 (d, J = 8.6 Hz, 2H), 8.00–7.93 (m, 3H), 7.74 (d, J = 15.6 Hz, 1H), 7.68 (d, J = 9.1 Hz, 1H), 7.43–7.38 (m, 1H), 7.31 (t, J = 8.6 Hz, 2H), 7.04 (t, J = 6.6 Hz, 1H). ^{13}C NMR (150 MHz, DMSO-d_6) δ 187.7, 161.5, 144.1, 143.5, 142.3, 139.3, 132.7, 131.4, 131.3, 129.9, 128.0, 127.0, 122.1, 119.7, 117.6, 116.2, 116.0, 113.7. HRMS (APCI): m/z calcd for $C_{23}H_{17}FN_3O_2^+$ $[M + H]^+$ 386.1299, found 386.1308.

4.2.2.11 | *(E)-N-(4-(3-(3,4-Dichlorophenyl)acryloyl) phenyl)imidazo[1,2-a]pyridine-2-carboxamide (**7 k**)*

Off-white solid, 187 mg (81% yield), mp: 269–270°C, ^{1}H NMR (600 MHz, DMSO-d_6) δ 10.69 (s, 1H), 8.64 (d, J = 6.4 Hz, 1H), 8.59 (s, 1H), 8.30 (s, 1H), 8.22 (d, J = 8.3 Hz, 2H), 8.15 (d, J = 8.2 Hz, 2H), 8.09 (d, J = 15.5 Hz, 1H), 7.88 (d, J = 7.8 Hz, 1H), 7.78–7.63 (m, 3H), 7.44–7.38 (m, 1H), 7.04 (t, J = 6.3 Hz, 1H).^{13}C NMR (150 MHz, DMSO-d_6) δ 187.5, 161.3, 143.9, 141.9, 139.1, 134.1, 132.4, 131.8, 130.7, 129.7, 129.2, 127.8, 126.8, 123.8, 122.8, 119.5, 119.4, 117.4, 116.0, 113.5. HRMS (APCI): m/z calcd for $C_{23}H_{16}Cl_2N_3O_2^+$ $[M + H]^+$ 436.0614, found 436.0620.

4.2.2.12 | *(E)-N-(4-(3-(4-Nitrophenyl)acryloyl) phenyl)imidazo[1,2-a]pyridine-2-carboxamide (**7 L**)*

Off-white solid, 159 mg (72% yield), mp: 305–306°C, ^{1}H NMR (600 MHz, DMSO-d_6) δ 10.70 (s, 1H), 8.64 (d, J = 6.2 Hz, 1H), 8.59 (s, 1H), 8.29 (d, J = 8.0 Hz, 2H), 8.24–8.15 (m, 6H), 7.81 (d, J = 15.7 Hz, 1H), 7.68 (d, J = 9.1 Hz, 1H), 7.44–7.38 (m, 1H), 7.05 (t, J = 6.1 Hz, 1H).^{13}C NMR (150 MHz, DMSO-d_6) 187.4, 161.3, 148.0, 143.9, 143.6, 141.4, 129.9, 129.8, 127.8, 126.8, 126.1, 123.9, 119.5, 117.4, 116.0, 113.6. HRMS (APCI): m/z calcd for $C_{23}H_{17}N_4O_4^+$ $[M + H]^+$ 413.1244, found 413.1261.

4.3 | Biology

4.3.1 | In vitro anti-parasitic assay

Anti-parasitic assays were performed as described in the earlier literature (Bouton et al., 2021). Briefly, to evaluate anti-*Leishmania* activity, *L. infantum* [MHOM/MA (BE)/67] was used with primary peritoneal mouse macrophages as host cell. 3×10^4 macrophages were infected with 4.5×10^5 parasites per well. Compound dilutions were added after 2 h of infection. After 5 days of incubation, parasite burdens (mean number of amastigotes/macrophage) were assessed microscopically after staining with a 10% Giemsa solution. For *T. cruzi*, the Tulahuen CL2, β-galactosidase strain (nifurtimox-sensitive) was used maintained on MRC-5_{SV2} (human lung fibroblast). 4×10^3 cells were infected with 4×10^4 parasites per well. Parasite burdens were assessed after adding the substrate CPRG (chlorophenol red ß-d-galactopyranoside). The change in colour was measured spectrophotometrically at 540 nm after 4 h incubation at 37°C. Drug susceptibility tests for *T. b. brucei* were performed using a resazurin assay. Susceptibility assays were performed with *T. b. brucei* Squib 427 or *T. b. rhodesiense* STIB-90050. *T. b. brucei* Squib 427 was seeded at 1.5×10^4 parasites/well and *T. b. rhodesiense* at 4×10^3 parasites per well, followed by the addition of resazurin after 72 h. Incubation with resazurin was for 24 h (*T. b. brucei*) or 6 h (*T. b. rhodesiense*) followed by fluorescence detection.

In all assays, parasite growth was compared to untreated-infected controls (100% growth) and noninfected controls (0% growth). Results were expressed as % parasite reduction at the different drug concentrations and used to calculate IC_{50} values from the dose–response curves.

4.3.2 | In-vitro cytotoxicity assay

MRC-5_{SV2} cell cytotoxicity was evaluated as described in the earlier literature (Bouton et al., 2021). Briefly, 1.5×10^5 cells/mL cells were cultured with compound dilutions at 37°C and with 5% CO_2. Cell growth was compared to untreated-control wells (100% cell growth) and medium-control wells (0% cell growth). After 3 days of incubation, cell viability was assessed fluorometrically after addition of 50-μL resazurin per well. After 4 h at 37°C, fluorescence was measured (λ_{ex} 550 nm, λ_{em} 590 nm). The results were expressed as % reduction in cell growth/viability compared to control wells and an IC_{50} value was determined.

ACKNOWLEDGEMENTS

DS Agarwal acknowledge North-West University, Potchefstroom Campus, South Africa for the post-doctoral funding. GC is a co-promotor of the 'Infla-Med' Centre of Excellence (www.uantwerpen.be/infla-med) and participates in COST Action CA21111.

CONFLICT OF INTEREST STATEMENT

The authors declare no conflicts of interest.

DATA AVAILABILITY STATEMENT

The data that supports the findings of this study are available in the supplementary material of this article (see Data S1).

ORCID

Lesetja J. Legoabe https://orcid.org/0000-0003-2440-4993

REFERENCES

Agarwal, D. S., Anantaraju, H. S., Sriram, D., Yogeeswari, P., Nanjegowda, S. H., Mallu, P., & Sakhuja, R. (2016). Synthesis, characterization and biological evaluation of bile acid-aromatic/heteroaromatic amides linked via amino acids as anti-cancer agents. *Steroids*, *107*, 87–97.

Agarwal, D. S., Krishna, V. S., Sriram, D., Yogeeswari, P., & Sakhuja, R. (2018). Clickable conjugates of bile acids and nucleosides: Synthesis, characterization, in vitro anticancer and antituberculosis studies. *Steroids*, *139*, 35–44.

Agarwal, D. S., Singh, R. P., Lohitesh, K., Jha, P. N., Chowdhury, R., & Sakhuja, R. (2018). Synthesis and evaluation of bile acid amides of α-cyanostilbenes as anticancer agents. *Molecular Diversity*, *22*(2), 305–321.

Almirante, L., Polo, L., Mugnaini, A., Provinciali, E., Rugarli, P., Biancotti, A., Gamba, A., & Murmann, W. (1965). Derivatives of imidazole. I. Synthesis and reactions of imidazo [1, 2-α] pyridines with analgesic, antiinflammatory, antipyretic, and anticonvulsant activity. *Journal of Medicinal Chemistry*, *8*(3), 305–312.

Bhambra, A. S., Ruparelia, K. C., Tan, H. L., Tasdemir, D., Burrell-Saward, H., Yardley, V., Beresford, K. J. M., & Arroo, R. R. (2017). Synthesis and antitrypanosomal activities of novel pyridylchalcones. *European Journal of Medicinal Chemistry*, *128*, 213–218.

Bischoff, F., Berthelot, D., De Cleyn, M., Macdonald, G., Minne, G., Oehlrich, D., Pieters, S., Surkyn, M., Trabanco, A. A., Tresadern, G., & Van Brandt, S. (2012). Design and synthesis of a novel series of bicyclic heterocycles as potent γ-secretase modulators. *Journal of Medicinal Chemistry*, *55*(21), 9089–9106.

Bouton, J., d'Almeida, A. F., Maes, L., Caljon, G., Van Calenbergh, S., & Hulpia, F. (2021). Synthesis and evaluation of 3′-fluorinated 7-deazapurine nucleosides as antikinetoplastid agents. *European Journal of Medicinal Chemistry*, *216*(113), 290.

Castera-Ducros, C., Paloque, L., Verhaeghe, P., Casanova, M., Cantelli, C., Hutter, S., Tanguy, F., Laget, M., Remusat, V., Cohen, A., & Crozet, M. D. (2013). Targeting the human parasite *Leishmania donovani*: Discovery of a new promising anti-infectious pharmacophore in 3-nitroimidazo [1, 2-a] pyridine series. *Bioorganic and Medicinal Chemistry*, *21*(22), 7155–7164.

Coulibaly, S., Evrard, A., Kumar, A., & Sissouma, D. (2023). Benzimidazoles and imidazo [1, 2-a] pyridines: Biological activities, method of synthesis and perspectives on combination of deuce, pharmacophore.

Croft, S., & Olliaro, P. (2011). Leishmaniasis chemotherapy—Challenges and opportunities. *Clinical Microbiology and Infection*, *17*(10), 1478–1483.

Davis, A., Cook, C., & Zumla, A. (2003). *Schistosomiasis: Manson's tropical diseases* (Vol. *21*, pp. 1431–1469). Elsevier Science.

De Rycker, M., Baragaña, B., Duce, S. L., & Gilbert, I. H. (2018). Challenges and recent progress in drug discovery for tropical diseases. *Nature*, *559*(7715), 498–506.

Deep, A., Kaur Bhatia, R., Kaur, R., Kumar, S., Kumar Jain, U., Singh, H., Batra, S., Kaushik, D., & Kishore Deb, P. (2017). Imidazo [1, 2-a] pyridine scaffold as prospective therapeutic agents. *Current Topics in Medicinal Chemistry*, *17*(2), 238–250.

Deschamps, P., Lara, E., Marande, W., López-García, P., Ekelund, F., & Moreira, D. (2011). Phylogenomic analysis of kinetoplastids supports that trypanosomatids arose from within bodonids. *Molecular Biology and Evolution*, *28*(1), 53–58.

Devi, N., Singh, D., Rawal, K., Bariwal, J., & Singh, V. (2016). Medicinal attributes of imidazo [1, 2-a] pyridine derivatives: An update. *Current Topics in Medicinal Chemistry*, *16*(26), 2963–2994.

Elkanzi, N. A., Hrichi, H., Alolayan, R. A., Derafa, W., Zahou, F. M., & Bakr, R. B. (2022). Synthesis of chalcones derivatives and their biological activities: A review. *ACS Omega*, *7*(32), 27769–27786.

Fersing, C., Basmaciyan, L., Boudot, C., Pedron, J., Hutter, S., Cohen, A., Castera-Ducros, C., Primas, N., Laget, M., Casanova, M., & Bourgeade-Delmas, S. (2018). Nongenotoxic 3-nitroimidazo [1, 2-a] pyridines are NTR1 substrates that display potent in vitro antileishmanial activity. *ACS Medicinal Chemistry Letters*, *10*(1), 34–39.

Fersing, C., Boudot, C., Castera-Ducros, C., Pinault, É., Hutter, S., Paoli-Lombardo, R., Primas, N., Pedron, J., Seguy, L., Bourgeade-Delmas, S., & Sournia-Saquet, A. (2020). 8-Alkynyl-3-nitroimidazopyridines display potent antitrypanosomal activity against both *T. b. brucei* and *cruzi*. *European Journal of Medicinal Chemistry*, *202*, 112558.

Fersing, C., Boudot, C., Pedron, J., Hutter, S., Primas, N., Castera-Ducros, C., Bourgeade-Delmas, S., Sournia-Saquet, A., Moreau, A., Cohen, A., & Stigliani, J. L. (2018).

8-Aryl-6-chloro-3-nitro-2-(phenylsulfonylmethyl) imidazo [1, 2-a] pyridines as potent antitrypanosomatid molecules bioactivated by type 1 nitroreductases. *European Journal of Medicinal Chemistry*, *157*, 115–126.

Field, M. C., Horn, D., Fairlamb, A. H., Ferguson, M. A., Gray, D. W., Read, K. D., De Rycker, M., Torrie, L. S., Wyatt, P. G., Wyllie, S., & Gilbert, I. H. (2017). Anti-trypanosomatid drug discovery: An ongoing challenge and a continuing need. *Nature Reviews Microbiology*, *15*(4), 217–231.

Goodacre, S. C., Street, L. J., Hallett, D. J., Crawforth, J. M., Kelly, S., Owens, A. P., Blackaby, W. P., Lewis, R. T., Stanley, J., Smith, A. J., & Ferris, P. (2006). Imidazo [1, 2-a] pyrimidines as functionally selective and orally bioavailable GABAAα2/α3 binding site agonists for the treatment of anxiety disorders. *Journal of Medicinal Chemistry*, *49*(1), 35–38.

Harrison, T. S., & Keating, G. M. (2005). Zolpidem: A review of its use in the management of insomnia. *CNS Drugs*, *19*, 65–89.

Lidani, K. C. F., Andrade, F. A., Bavia, L., Damasceno, F. S., Beltrame, M. H., Messias-Reason, I. J., & Sandri, T. L. (2019). Chagas disease: From discovery to a worldwide health problem. *Frontiers in Public Health*, *7*, 166.

Mathias, F., Cohen, A., Kabri, Y., Negrão, N. W., Crozet, M. D., Docampo, R., Azas, N., & Vanelle, P. (2020). Synthesis and in vitro evaluation of new 5-substituted 6-nitroimidazooxazoles as antikinetoplastid agents. *European Journal of Medicinal Chemistry*, *191*(112), 146.

Molyneux, D. H., Savioli, L., & Engels, D. (2017). Neglected tropical diseases: Progress towards addressing the chronic pandemic. *The Lancet*, *389*(10066), 312–325.

Nava-Zuazo, C., Chávez-Silva, F., Moo-Puc, R., Chan-Bacab, M. J., Ortega-Morales, B. O., Moreno-Díaz, H., Díaz-Coutiño, D., Hernández-Núñez, E., & Navarrete-Vázquez, G. (2014). 2-acylamino-5-nitro-1, 3-thiazoles: Preparation and in vitro bioevaluation against four neglected protozoan parasites. *Bioorganic and Medicinal Chemistry*, *22*(5), 1626–1633.

Patterson, S., & Wyllie, S. (2014). Nitro drugs for the treatment of trypanosomatid diseases: Past, present, and future prospects. *Trends in Parasitology*, *30*(6), 289–298.

Pillay-van Wyk, V., & Bradshaw, D. (2017). Mortality and socioeconomic status: The vicious cycle between poverty and ill health. *The Lancet Global Health*, *5*(9), e851–e852.

Povelones, M. L. (2014). Beyond replication: Division and segregation of mitochondrial DNA in kinetoplastids. *Molecular and Biochemical Parasitology*, *196*(1), 53–60.

Rammohan, A., Reddy, J. S., Sravya, G., Rao, C. N., & Zyryanov, G. V. (2020). Chalcone synthesis, properties and medicinal applications: A review. *Environmental Chemistry Letters*, *18*, 433–458.

Reddy, P. V., Hridhay, M., Nikhil, K., Khan, S., Jha, P., Shah, K., & Kumar, D. (2018). Synthesis and investigations into the anticancer and antibacterial activity studies of β-carboline chalcones and their bromide salts. *Bioorganic and Medicinal Chemistry Letters*, *28*(8), 1278–1282.

Reddyrajula, R., & Dalimba, U. K. (2019). Structural modification of zolpidem led to potent antimicrobial activity in imidazo [1, 2-a] pyridine/pyrimidine-1, 2, 3-triazoles. *New Journal of Chemistry*, *43*(41), 16281–16299.

Robinson, W. J., Taylor, A. E., Lauga-Cami, S., Weaver, G. W., Arroo, R. R., Kaiser, M., Gul, S., Kuzikov, M., Ellinger, B., Singh, K., & Schirmeister, T. (2021). The discovery of novel antitrypanosomal 4-phenyl-6-(pyridin-3-yl) pyrimidines. *European Journal of Medicinal Chemistry*, *209*(112), 871.

Salehi, B., Quispe, C., Chamkhi, I., El Omari, N., Balahbib, A., Sharifi-Rad, J., Bouyahya, A., Akram, M., Iqbal, M., Docea, A. O., & Caruntu, C. (2021). Pharmacological properties of chalcones: A review of preclinical including molecular mechanisms and clinical evidence. *Frontiers in Pharmacology*, *11*(592), 654.

Singhaus, R. R., Bernotas, R. C., Steffan, R., Matelan, E., Quinet, E., Nambi, P., Feingold, I., Huselton, C., Wilhelmsson, A., Goos-Nilsson, A., & Wrobel, J. (2010). 3-(3-Aryloxyaryl) imidazo [1, 2-a] pyridine sulfones as liver X receptor agonists. *Bioorganic and Medicinal Chemistry Letters*, *20*(2), 521–525.

Stuart, K., Brun, R., Croft, S., Fairlamb, A., Gürtler, R. E., McKerrow, J., Reed, S., & Tarleton, R. (2008). Kinetoplastids: Related protozoan pathogens, different diseases. *The Journal of Clinical Investigation*, *118*(4), 1301–1310.

Tresadern, G., Cid, J. M., Macdonald, G. J., Vega, J. A., de Lucas, A. I., García, A., García, A., Matesanz, E., Linares, M. L., Oehlrich, D., Lavreysen, H., & Biesmans, I. (2010). Scaffold hopping from pyridones to imidazo [1, 2-a] pyridines. New positive allosteric modulators of metabotropic glutamate 2 receptor. *Bioorganic and Medicinal Chemistry Letters*, *20*(1), 175–179.

Wyllie, S., Patterson, S., Stojanovski, L., Simeons, F. R., Norval, S., Kime, R., Read, K. D., & Fairlamb, A. H. (2012). The anti-trypanosome drug fexinidazole shows potential for treating visceral leishmaniasis. *Science Translational Medicine*, *4*(119), 119re111.

Zhao, Y. H., Abraham, M. H., Le, J., Hersey, A., Luscombe, C. N., Beck, G., Sherborne, B., & Cooper, I. (2002). Rate-limited steps of human oral absorption and QSAR studies. *Pharmaceutical Research*, *19*, 1446–1457.

Zulfiqar, B., Shelper, T. B., & Avery, V. M. (2017). Leishmaniasis drug discovery: Recent progress and challenges in assay development. *Drug Discovery Today*, *22*(10), 1516–1531.

SUPPORTING INFORMATION

Additional supporting information can be found online in the Supporting Information section at the end of this article.

How to cite this article: Agarwal, D. S., Beteck, R. M., Ilbeigi, K., Caljon, G., & Legoabe, L. J. (2024). Design and synthesis of imidazo[1,2-*a*] pyridine-chalcone conjugates as antikinetoplastid agents. *Chemical Biology & Drug Design*, *103*, e14400. https://doi.org/10.1111/cbdd.14400